Supporting Information

Nitrous Oxide and Methane Dynamics in Woodchip Bioreactors: Effects of Water Level Fluctuations on Gas Partitioning into Trapped Gas Phases

Philip M. McGuire and Matthew C. Reid

School of Civil and Environmental Engineering, Cornell University, Ithaca NY 14853, USA

Number of Pages: 31

Number of Tables: 3

Number of Figures: 17

Summary

Model Description

Equilibrium Dissolved Gas Transport in the Presence of Trapped Gas Phases

Small volumes of trapped gas bubbles in otherwise saturated media can significantly retard the transport of sparingly soluble gases. Gases partition from the aqueous phase into bubble phases when gas concentrations in bubbles are undersaturated with respect to equilibrium with the aqueous phase, while bubbles serve as sources of gases to water when bubbles are supersaturated relative to the aqueous phase. One-dimensional transport of a dissolved gas through a porous media with trapped gas phases can be described with (Fry et al.;):

$$R\frac{\partial c_m}{\partial t} = D\frac{\partial^2 c_m}{\partial x^2} - v\frac{\partial c_m}{\partial x} \qquad (S1)$$

where c_m = concentration of dissolved gas in the mobile aqueous phase; t = time; D = dispersion coefficient; x = distance; v = porewater velocity; and R = retardation factor, which is defined as:

$$R = 1 + H\frac{V_g}{V_w} \qquad (S2)$$

where H = dimensionless Henry's Law Constant (Table 1); V_g = volume of gas-filled pore space; and V_w = volume of water-filled pore space. This model effectively describes transport of dissolved gases through porous media when gases in bubble and mobile water phases are in equilibrium[1,3], but fails to describe dissolved gas transport when mass transfer limitations lead to nonequilibrium conditions between the phases[2,4,5].

Non-equilibrium Dissolved Gas Transport in the Presence of Trapped Gas Phases

Non-equilibrium gas transport in the presence of trapped bubbles can be described with a one-site advection-dispersion-mass transfer model[2]:

$$\frac{\partial c_m}{\partial t} + \frac{V_g}{V_w}\frac{\partial c_g}{\partial t} = D\frac{\partial^2 c_m}{\partial x^2} - v\frac{\partial c_m}{\partial x} \qquad (S3)$$

Where c_g = concentration of gas in the gaseous phase and

$$\frac{\partial c_g}{\partial t} = \alpha\left(Hc_w - c_g\right) \qquad (S4)$$

α is a first-order mass transfer rate coefficient [T^{-1}] and here, describes the assumed diffusion-limited transfer of gas from the mobile water phase to the immobile gaseous phase. Dimensionless variables can be introduced and eqn. (S3) can be reduced to the dimensionless form:

$$\beta R\frac{\partial c_1}{\partial \mathrm{T}} + (1-\beta)R\frac{\partial c_2}{\partial \mathrm{T}} = \frac{1}{P}\frac{\partial^2 c_1}{\partial z^2} - \frac{\partial c_1}{\partial \mathrm{z}} \qquad (S5)$$

Where:

$$(1-\beta)R\frac{\partial c_2}{\partial \mathrm{T}} = \omega(c_1 - c_2) \qquad (S6)$$

In this dimensionless form of the model, the dimensionless parameters c_1, c_2, T, z, P, ω, and β are defined as:

$$c_1 = \frac{c_w}{c_w^0} \qquad (S7a)$$

$$c_2 = \frac{c_g}{Hc_w^0} \qquad (S7b)$$

$$T = \frac{vt}{L} \tag{S7c}$$

$$z = \frac{x}{L} \tag{S7d}$$

$$P = \frac{vL}{D} \tag{S7e}$$

$$\omega = \frac{\alpha L(R-1)}{v} \tag{S7f}$$

$$\beta = \frac{1}{R} \tag{S7g}$$

c_1 = normalized dissolved gas concentration in the aqueous phase; c_w = dissolved gas concentration in the aqueous phase; c_w^0 = dissolved gas concentration in the tracer solution at the reactor inlet; c_2= normalized gas concentration in immobile bubbles; T = reactor pore volumes; and z = distance normalized to reactor length (L).

Dual Porosity Non-Equilibrium Dissolved Gas Transport

Solute transport in porous media is often influenced by transfer of solutes between mobile and immobile, or stagnant, water volumes[6] and trapped gas phases may be located in either the mobile or stagnant water volume. Such dual-porosity models have recently been proposed for solute transport in woodchip porous media[7], with water inside woodchips treated as the stagnant volume while water in the interpore structure between woodchips is treated as the mobile water volume. Dissolved gas transport in a dual-porosity system with trapped bubbles located in both stagnant and mobile domains can be described using:

$$\theta_m \frac{\partial c_m}{\partial \mathrm{t}} + \frac{V_{g,m}}{V_{w,m}} \frac{\partial c_{g,m}}{\partial \mathrm{t}} + \theta_{im} \frac{\partial c_{im}}{\partial \mathrm{t}} + \frac{V_{g,im}}{V_{w,im}} \frac{\partial c_{g,im}}{\partial \mathrm{t}} = \theta_m D \frac{\partial^2 c_m}{\partial x^2} - \theta_m v \frac{\partial c_m}{\partial \mathrm{x}} \qquad (S8)$$

Where Θ_m = porosity of the mobile phase; c_m = dissolved gas concentration in the mobile phase; $V_{g,m}/V_{w,m}$ = ratio of bubble volume to water volume in mobile phase; $c_{g,m}$ = gas concentration in bubbles entrapped in the mobile phase; Θ_{im} = porosity of the immobile phase; c_{im} = dissolved gas concentration in the immobile phase; $V_{g,im}/V_{w,im}$ = ratio of bubble volume to water volume in immobile phase; and $c_{g,im}$ = gas concentration in bubbles entrapped in the immobile phase.

Eqn. (S8) can be reduced to the same form as eqn. (S5), but with changes in some dimensionless variables defined as:

$$c_2 = \frac{c_{im}}{c_w^0} \qquad (S9a)$$

$$T = \frac{v_m t}{L} \qquad (S9b)$$

$$z = \frac{x}{L} \qquad (S9c)$$

$$P = \frac{v_m L}{D} \qquad (S9d)$$

$$\omega = \frac{\alpha L}{\theta_m v_m} \qquad (S9e)$$

$$\beta = \frac{\Phi_m R_m}{R} \qquad (S9f)$$

Where c_{im} = the dissolved gas concentration in the immobile aqueous phase within the media; v_m = velocity of the mobile phase; φ_m = the mobile aqueous fraction ($\Theta_m/(\Theta_m+\Theta_{im})$; and R_m = the

retardation factor due to trapped bubbles in the mobile domain. From this simplification, L is measured based on the dimensions of the reactor and Θ_m is measured based on the reactor's drainable porosity (see Section 3.1). v_m and D are determined using bromide as a nonvolatile, non-sorbing tracer. α, R, and R_m can be determined for each dissolved gas tracer. Here, α is once again assumed as diffusion controlled, but now describes exchange between the mobile aqueous fraction to the immobile aqueous domain. R_m is determined using the equation:

$$R_m = 1 + H\frac{V_{g,m}}{V_{w,m}} \qquad (S10)$$

While different gases moving through the same reactor will be characterized by different R or R_m values, the corresponding V_g/V_w or $V_{g,m}/V_{w,m}$ values (calculated using eqn. S2 or eqn. S10) should be the same since these ratios are a physical property of the reactor.

Methods

Dissolved Gas Tracer Tests

The tracer solution was prepared by filling a collapsible polyethylene bag with Milli-Q water and adding bromide (Br^-) and sodium azide (NaN_3) to final concentrations of 5 mM Br^- and 50 mM NaN_3 – NaN_3 was omitted in the biotic cases. This solution was then bubbled with helium for one hour. A separate collapsible gas bag with dissolved ethane, SF_6, CH_4, and N_2O was prepared by filling the headspace with the gases and mixing. After agitation, the dissolved gas blend was added to the larger tracer solution. Residual headspace within the solution bag was forced out

and the container was sealed and submerged in a water bath to reduce potential losses of gases from the solution during the experiment.

Sampling and Analysis

Water samples were collected using glass syringes, and care was taken to ensure that no bubbles were collected in the syringe. For GC analysis prep, approximately 4 mL of water was displaced from the vials by N_2 to create a headspace for quantification via GC analysis (Shimadzu GC-2014 with an AOC-5000 autosampler). N_2O and SF_6 were measured using an electron capture detector, He was measured with a thermal conductivity detector, and CH_4 and C_2H_6 measured with a flame ionization detector.

X-Ray Computed Microtomography

2401 projections were recorded for each scan. Beam energy was set to 100kV/9W with a resolution of 3.5-4 microns per voxel and an exposure time of between 1 and 2 seconds, adjusted for each to account for the increased density of the stained samples. The total imaged volume was a cylinder 999 voxels in diameter and 999 voxels in height.

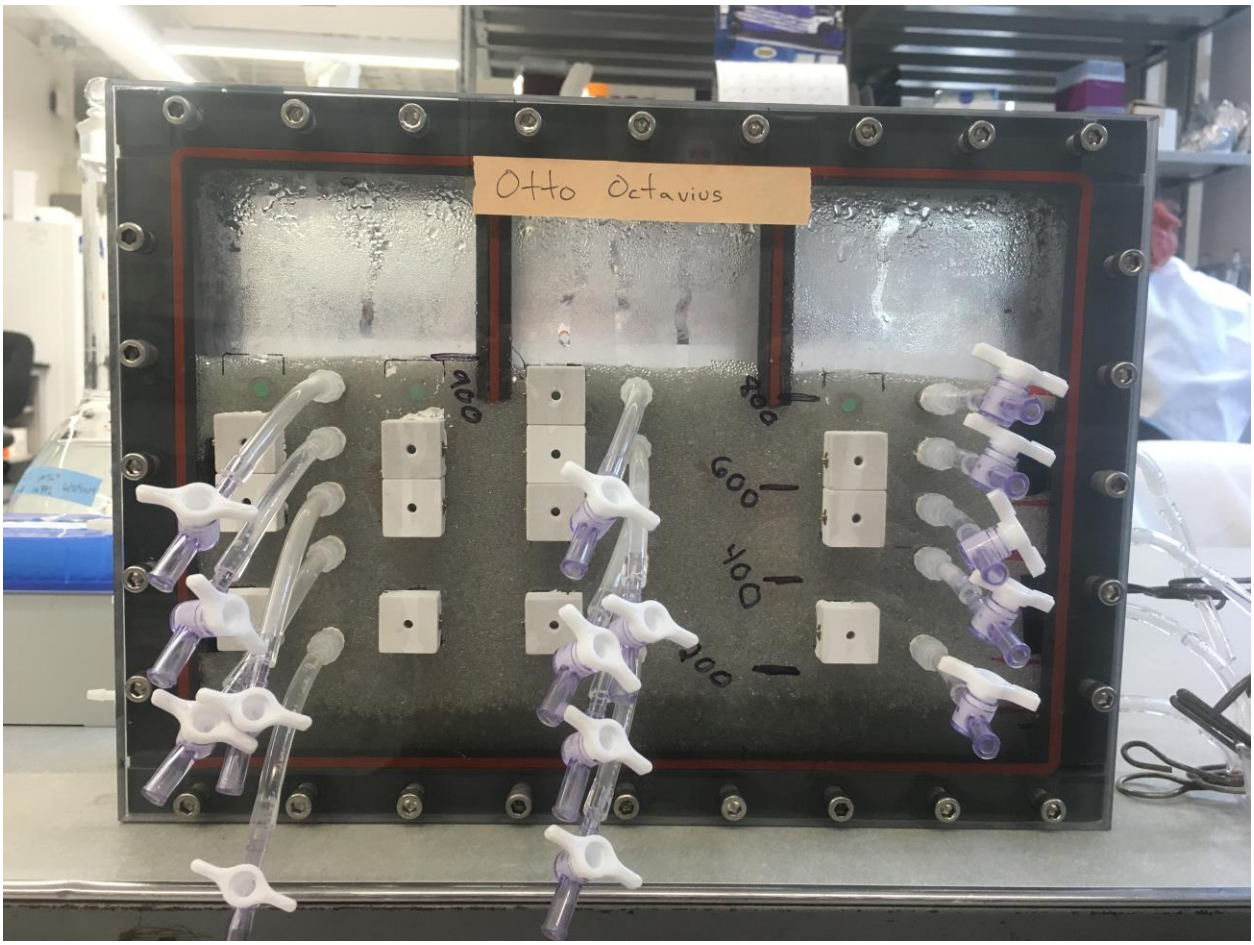

Figure S1: Front view of reactor packed with glass beads

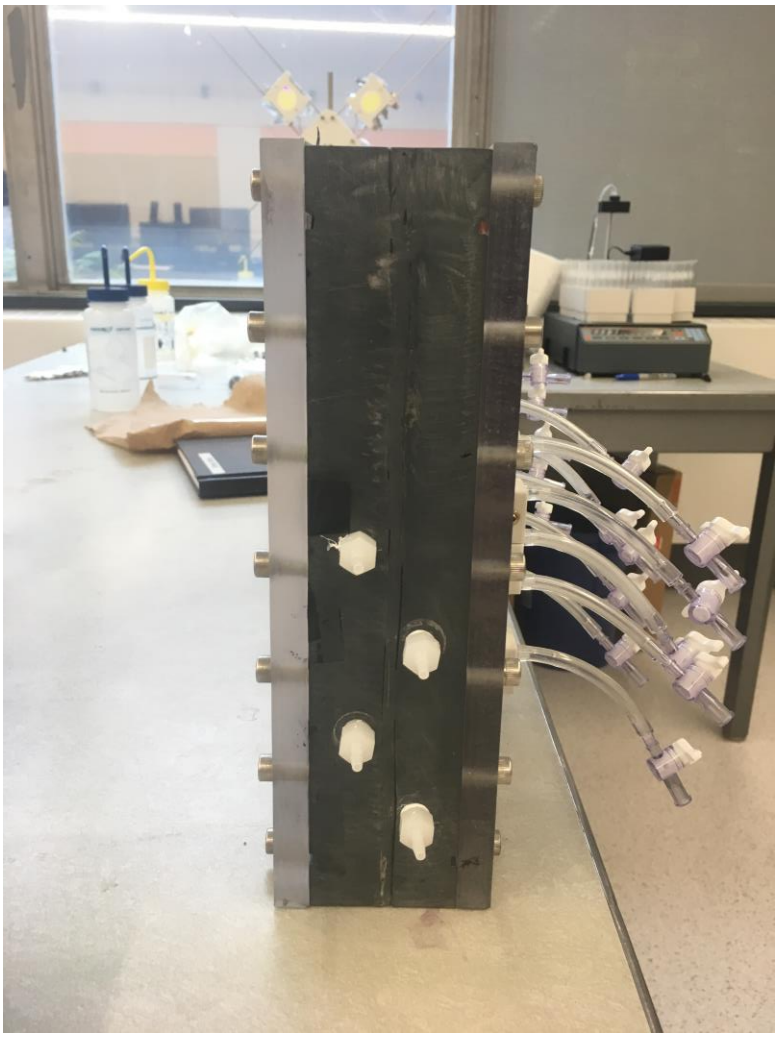

Figure S2: Reactor Side View

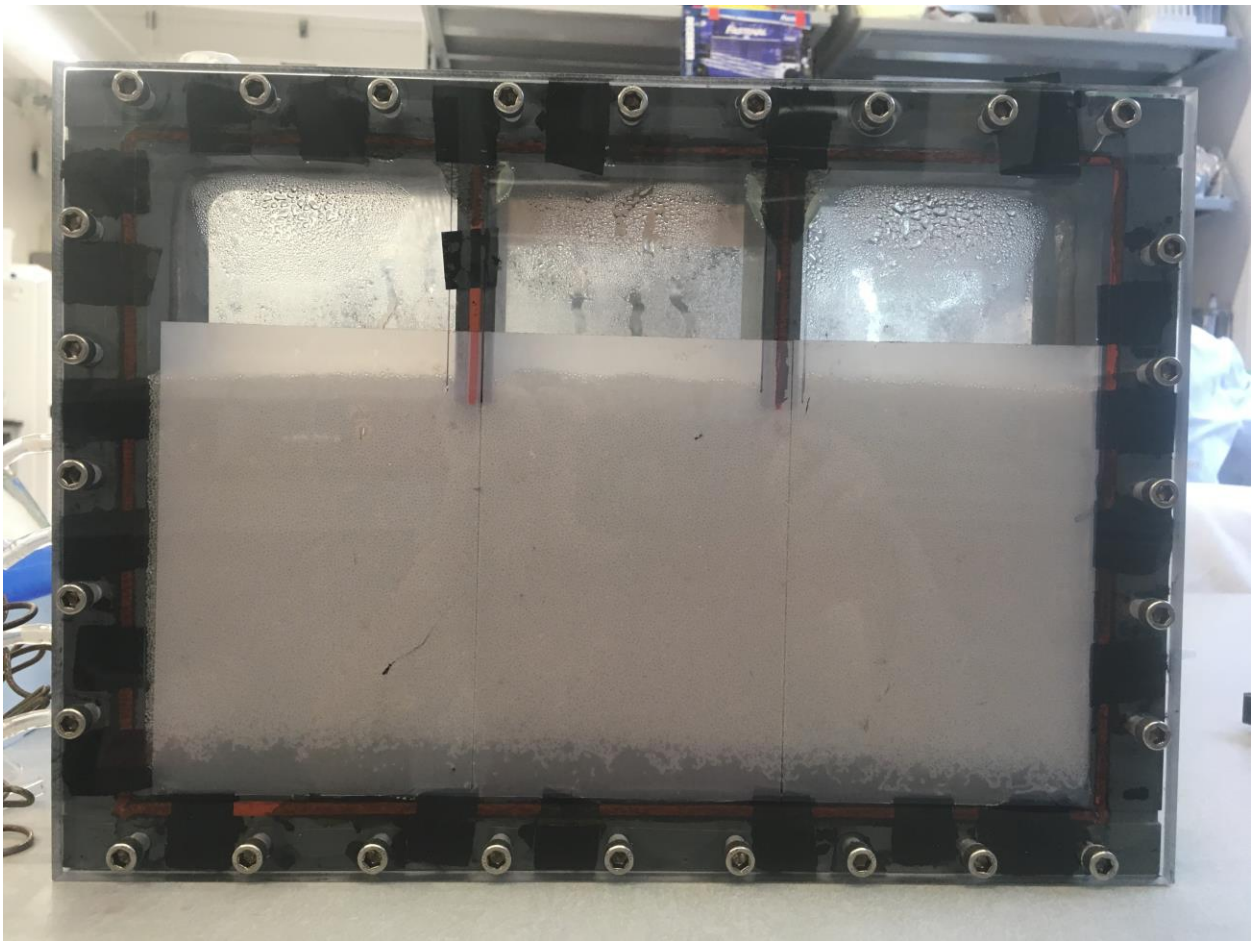

Figure S3: Reactor Rear View

Table S1: Physical-Chemical Properties of Gases at 25°C[8–10]

Table 1: **Dissolved Gas Properties**

Gas	**Water D [1×10^{-5} cm^2/s]**	**H [dimensionless]**
N_2O	2.10	1.68
Ethane	1.38	22.1
Methane	1.67	27.3
Helium	6.28	106
SF_6	1.20	168

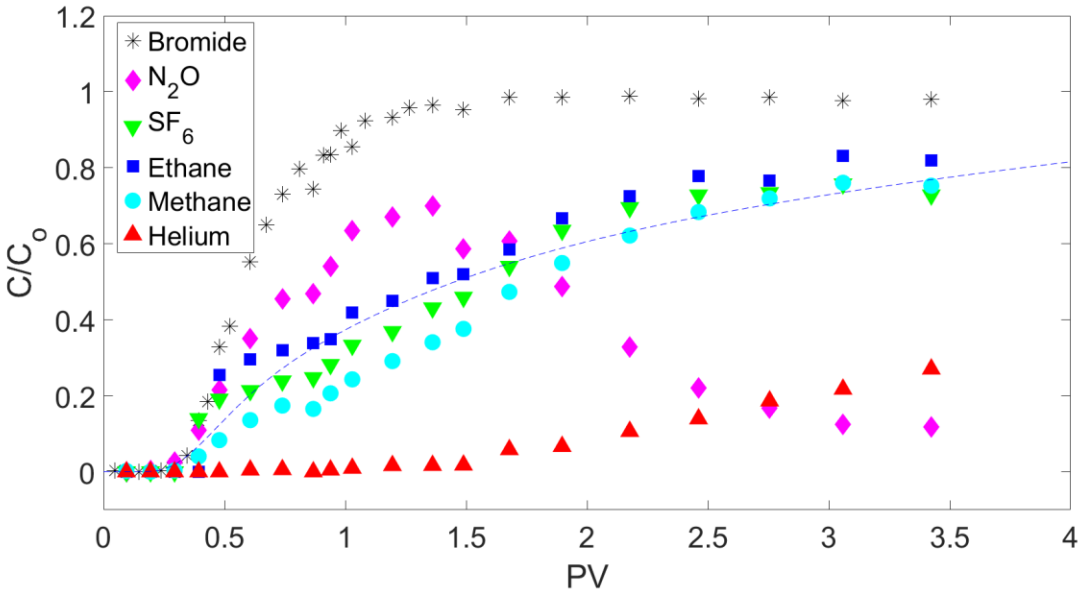

Figure S4: Model Validation with Ethane. Ethane breakthrough is simulated with the dashed blue line, and this is compared to ethane measurements (blue squares). Overall V_g/V_w within the system is taken as the average of overall V_g/V_w values estimated from SF_6 and He. $V_g/V_{w,m}$ values were fit for He and SF_6 and a linear relationship between gas diffusivity and $V_{g,m}/V_{w,m}$ was established for interpolation of ethane. The α value was taken as an average of α from replicate abiotic experiments subjected to identical antecedent hydrologic conditions.

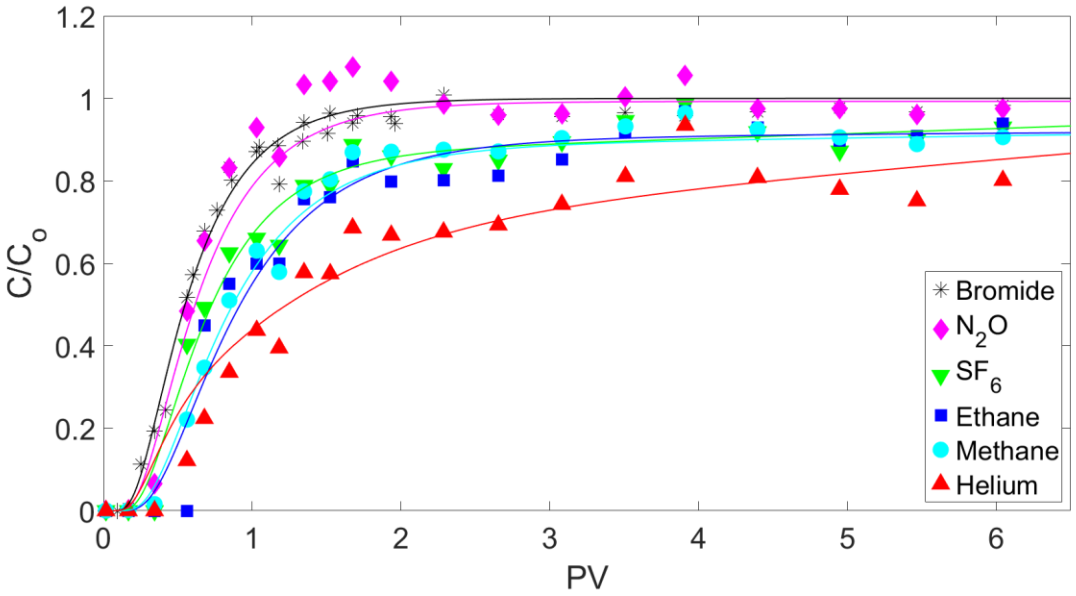

Figure S5: Duplicate Abiotic, Static Woodchip Experiment

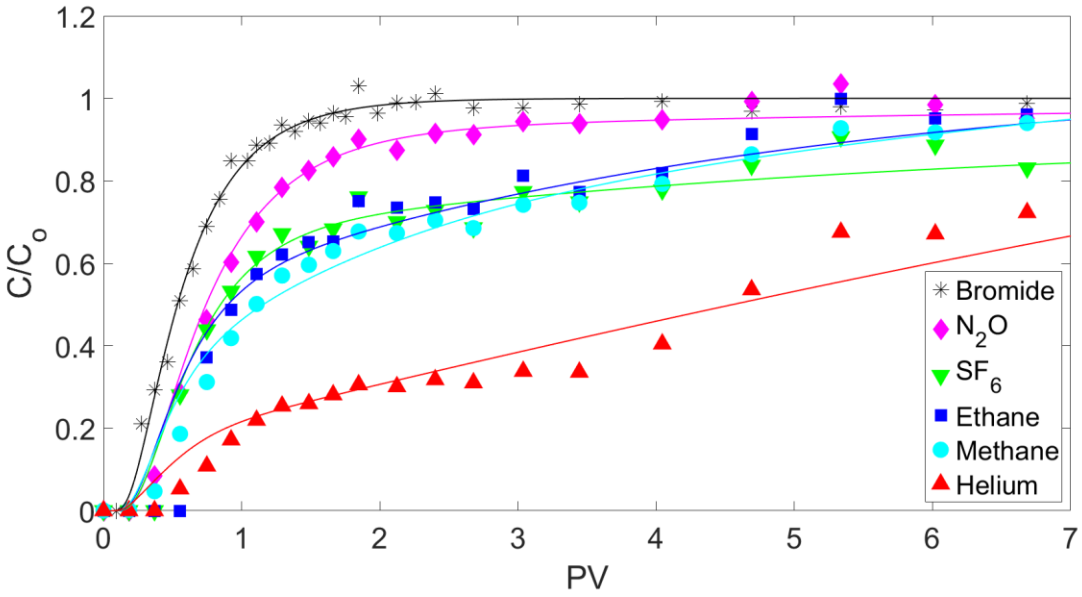

Figure S6: Duplicate, Abiotic, Transient Woodchip Experiment

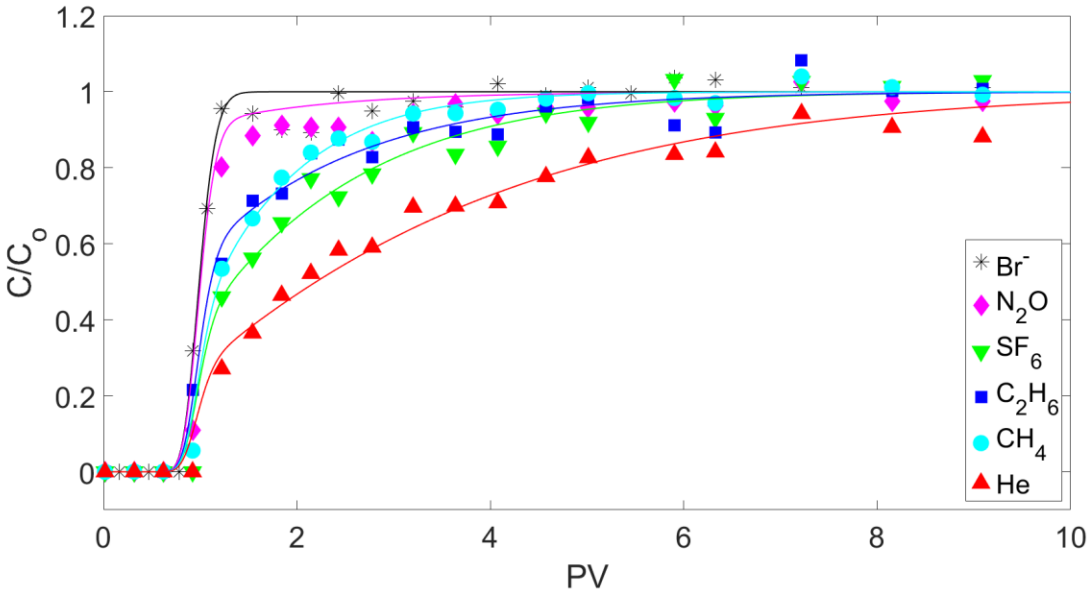

Figure S7: Duplicate, Abiotic, Transient Glass Bead Experiment

Table S2: Model Parameters α, R, and R_m															
Experiment	**α ×10^{-5} (s^{-1})**					**R**					**R_m**				
Gas	N_2O	CH_4	C_2H_6	He	SF_6	N_2O	CH_4	C_2H_6	He	SF_6	N_2O	CH_4	C_2H_6	He	SF_6
Glass Beads 1	20	22	17	15	12	1.09	1.55	1.61	3	2.1	N/A	N/A	N/A	N/A	N/A
Glass Beads 2	20	40	20.5	15.5	24.5	1.11	1.54	1.68	3.12	1.95	N/A	N/A	N/A	N/A	N/A
Abiotic, Stable 1	2.4	0.55	0.55	0.95	0.08	1.18	3.9	3.5	15.8	18	1.08	1.3	1.6	1.05	1.3
Abiotic, Stable 2	0.60	0.66	0.55	1.11	0.11	1.16	3.4	3.4	15.9	17.2	1.12	1.5	1.6	1.03	1.25
Abiotic, Transient 1	9.40	1.60	1.68	2.4	0.14	1.35	7	6.1	21	48.8	1.2	1.19	1.23	1.01	1.18
Abiotic, Transient 2	3.0	2.25	1.58	4.0	0.11	1.36	6.9	6	17	47.5	1.34	1.15	1.21	1.01	1.3
Biotic, Transient 1	6.2	1.92	1.20	0.11	0.14	1.58	11.2	8.5	39	57.5	1.00	1.01	1.01	6.1	1.01
Biotic, Transient 2	6.2	1.92	1.20	0.04	0.19	1.6	11.6	9.15	40	57.5	1.00	1.01	1.01	7.01	1.01

Table S3: Estimated V_g/V_w and $V_g/V_{w,m}$ Values										
Experiment	**V_g/V_w**					**$V_{g,m}/V_{w,m}$**				
Gas	N_2O	CH_4	C_2H_6	He	SF_6	N_2O	CH_4	C_2H_6	He	SF_6
Glass Beads 1	0.0536	0.0186	0.0276	0.0189	0.00655	N/A	N/A	N/A	N/A	N/A
Glass Beads 2	0.0655	0.0183	0.308	0.0201	0.00565	N/A	N/A	N/A	N/A	N/A
Abiotic, Stable 1	0.107	0.106	0.113	0.140	0.101	0.0476	0.0110	0.0271	4.72E-4	0.00179
Abiotic, Stable 2	0.0952	0.0879	0.109	0.140	0.0964	0.0714	0.0183	0.0271	2.83E-4	0.00149
Abiotic, Transient 1	0.208	0.203	0.231	0.189	0.284	0.119	0.00627	0.0102	9.46E-5	0.00104
Abiotic, Transient 2	0.214	0.200	0.226	0.151	0.277	0.202	0.00508	0.00950	9.46E-5	0.00179
Biotic, Transient 1	0.345	0.345	0.334	0.360	0.336	2.56E-4	2.56E-4	4.52E-4	0.0482	5.95E-5
Biotic, Transient 2	0.357	0.357	0.369	0.369	0.336	2.56E-4	2.56E-4	4.52E-4	0.0569	5.95E-5

Mass Balance Calculations

Mass balances within a breakthrough curve context were generated as follows: mass attributed to effluent discharge was determined as the area under the modeled breakthrough curve of a given dissolved gas (Figure S8) normalized by the area of injected mass within an experiment (Figure S9). For a step input (normalized as C/C0) this injected mass area will equal the number of pore volumes injected during the experiment (#PVs x injected normalized concentration [1]). The area under a modeled breakthrough curve was taken as the integral of the breakthrough curve between the bounds of 0 and the number of pore volume injections + 1 (the additional PV represents the volume of water drained at the conclusion of the experiment). Mass attributed to retention in the reactor (both headspace and bubble entrapped mass) was determined as the area between bromide and dissolved gas breakthrough curves (Figure S10) normalized by the area of injected mass.

Mass balances calculated from direct measurements were generated as follows: effluent, headspace prior to drainage, and headspace post-drainage values were all quantified via GC analysis. The summed mass in each of these compartments was then normalized by the total mass injected into the reactor. Mass injected into the reactor was determined by quantification of influent samples collected approximately every 2 hours during the experiment. Linear interpolation between these data points generated a series of the tracer solution concentration over time. For every time (or pore volume) step in the fitted model of each gas (~1000 discretizations for each experiment) the average of the tracer solution concentrations bounding the time step of interest was multiplied by the volume injected during that time segment to obtain the mass injected during that period. Summation of the masses injected over all periods is the

total mass of each dissolved gas injected into the reactor. Effluent, headspace prior to drainage, and headspace post-drainage masses were all normalized by this total mass injection.

Following normalization to the total mass injected, the direct measurement normalized effluent value was equated with the effluent mass discharged in the breakthrough curve-based mass balance approach. The fractional change between the measured and modeled effluent values was multiplied by the normalized values of the headspace prior to- and post-drainage. This normalizes all direct measurement mass balances within the context of the breakthrough curve mass balances and permits comparison of modeled and experimental approaches.

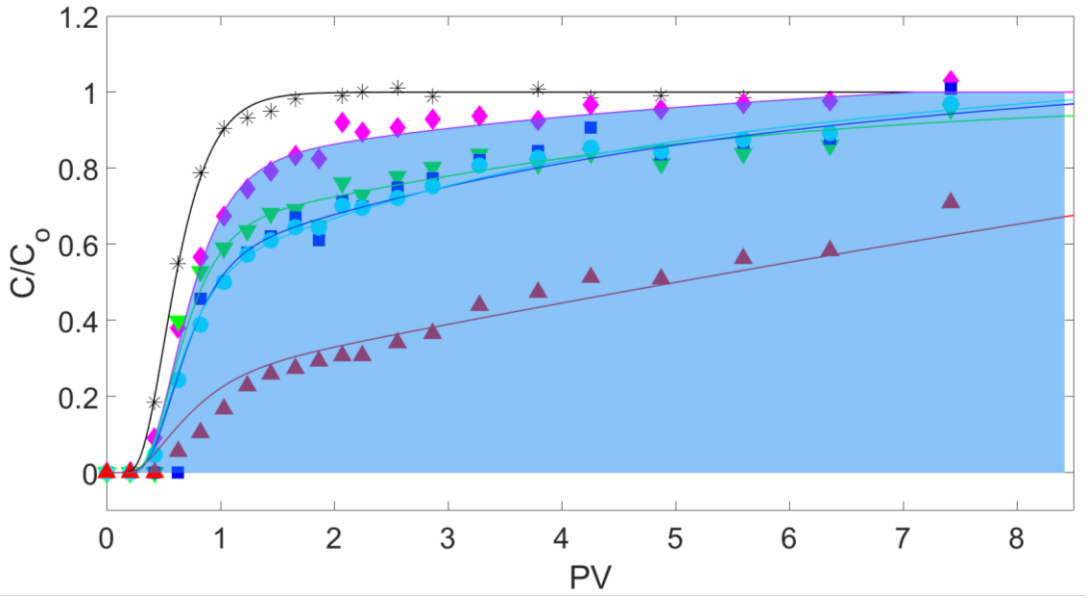

Figure S8: Effluent Mass Graphic. Illustration of determining effluent mass exported from the reactor for breakthrough curve-based mass balances.

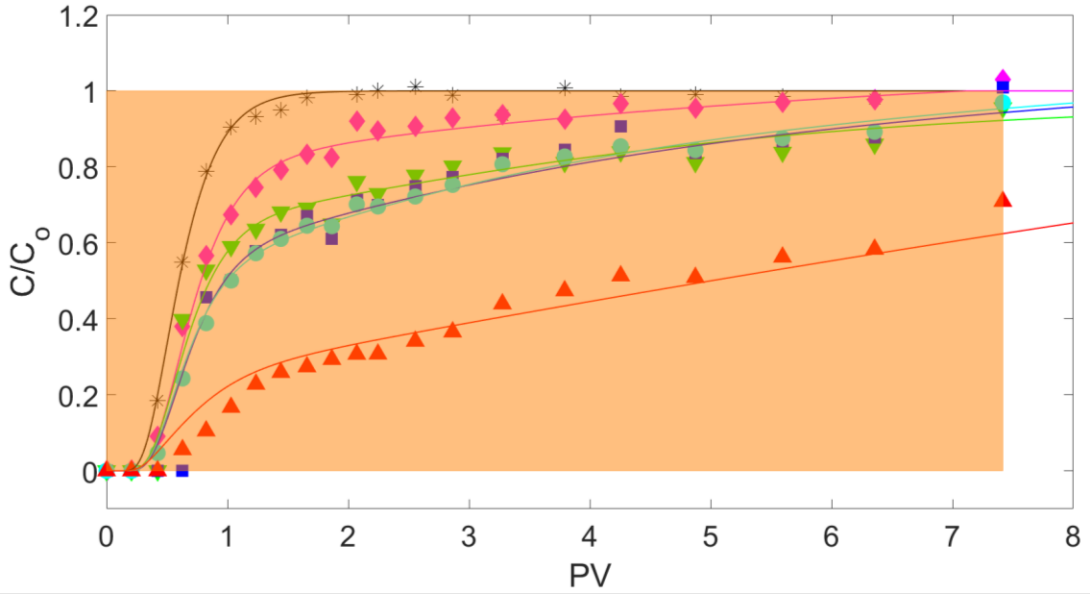

Figure S9: Injected Mass Graphic. Illustration of determining total mass injected into the reactor for breakthrough curve-based mass balances.

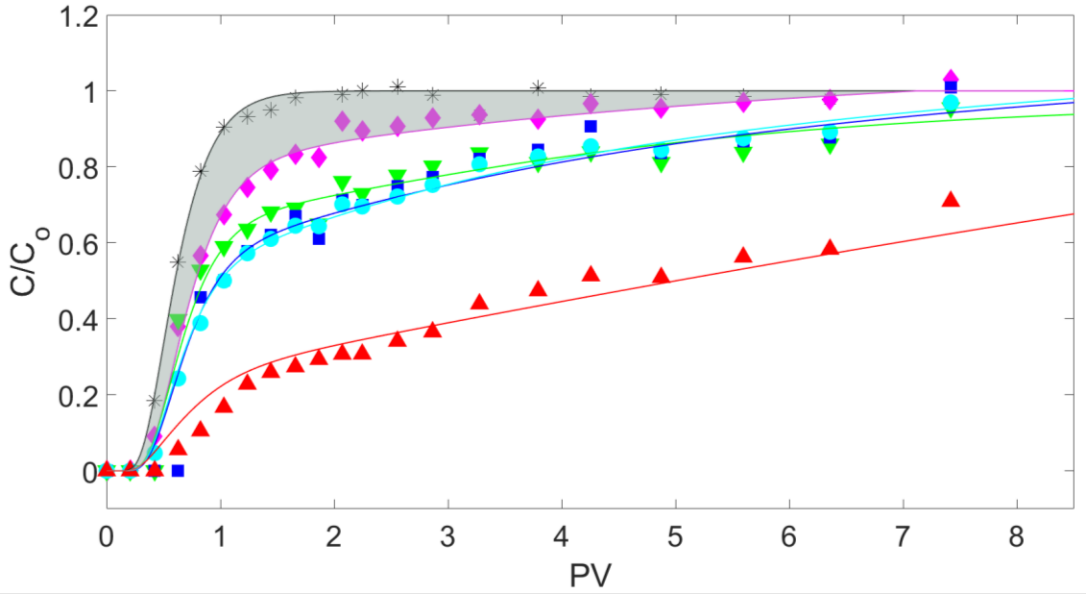

Figure S10: Retained Mass Graphic. Illustration of determining mass retained within the reactor for breakthrough curve-based mass balances.

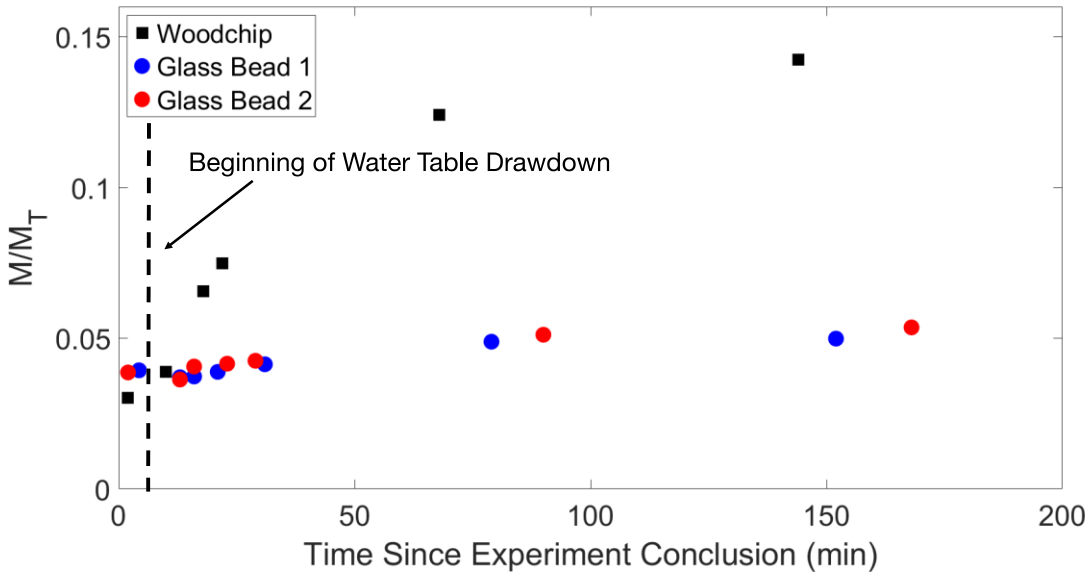

Figure S11: N_2O headspace mass as a function of time following reactor drainage at the end of an abiotic transient tracer experiment. M/M_T is the mass of N_2O measured in the reactor headspace normalized by the total mass injected into the reactor.

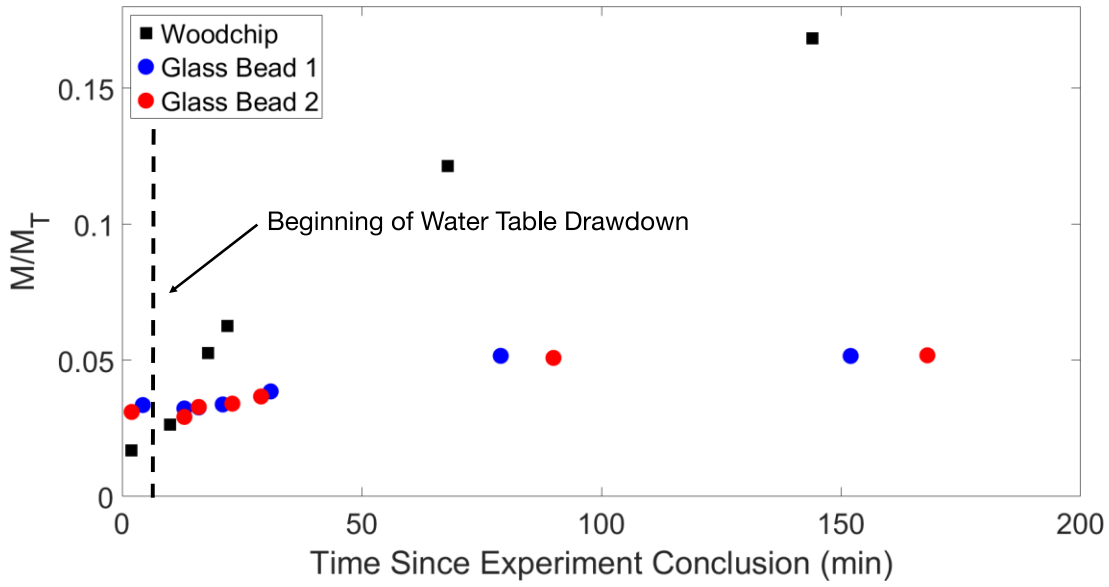

Figure S12: CH_4 headspace mass as a function of time following reactor drainage at the end of an abiotic transient tracer experiment. M/M_T is the mass of CH_4 measured in the reactor headspace normalized by the total mass injected into the reactor.

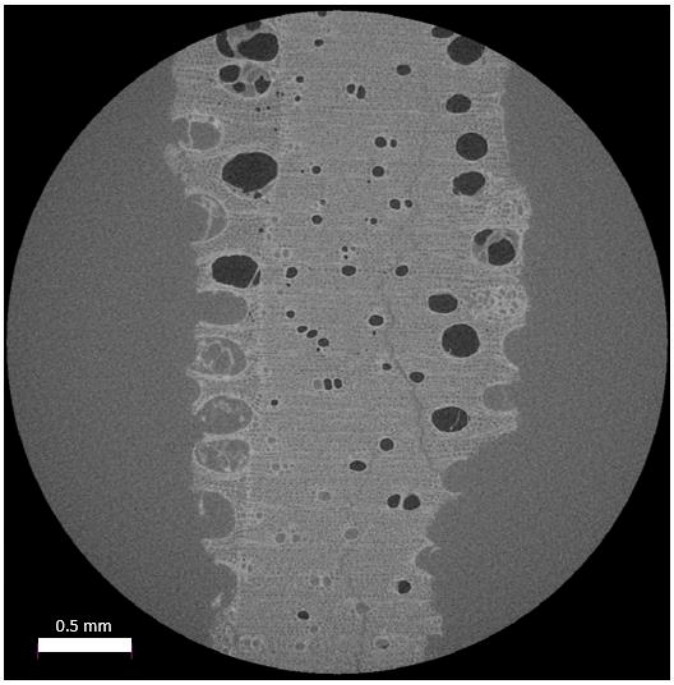

Figure S13: μCT image slice of woodchip soaked in 3% iodine solution for one week. Dark circles are indicative of bubbles entrapped within woodchip intraporosity.

V_g/V_t Calculations

Measured Values: Total Porosity = 0.90

Measured Saturated Media Volume = ~1620 mL

Measured Drainable Water Volume = ~1050 mL

Example Transient Case $V_g/V_w = 0.151$

To allow for a comparison of experimental μCT results (V_g/V_t) and the modeled reactor property V_g/V_w, these properties must be expressed in the same terms. The following describes the transformation of V_g/V_w to V_g/V_t.

We define V_t as the volume taken up by a woodchip and including the water and air pockets located in the intraporosity of the woodchip. Within the μCT scans, this encompasses all phases excluding the bulk iodine solution. In the reactor, this will equal the volume of the saturated media volume minus the drainable water volume:

$$V_t: \quad 1620\ mL - 1050\ mL = 570\ mL$$

Next we must determine V_g from our V_g/V_w value of 0.151. We know that the total porosity of the system is 0.9 but cannot state that 0.9 is comprised entirely of water – it may also contain trapped gas volume. Using the porosity and total saturated media volume, we determine V_w^* to be:

$$V_w^*: \quad 0.9 \times 1620\ mL = 1458\ mL$$

where V_w^* is defined as the volume of water (V_w) and gas (V_g) within the system. Solving for V_w then gives us:

$$V_w = 1458 - V_g$$

We can then plug our V_w into $V_g/V_w = 0.151$ to solve for V_g.

$$\frac{V_g}{1458 - V_g} = 0.151$$

Giving us V_g = 191 mL. Using our acquired value of V_g and our previously determined value of V_t, we find:

$$\frac{V_g}{V_t} = 0.34$$

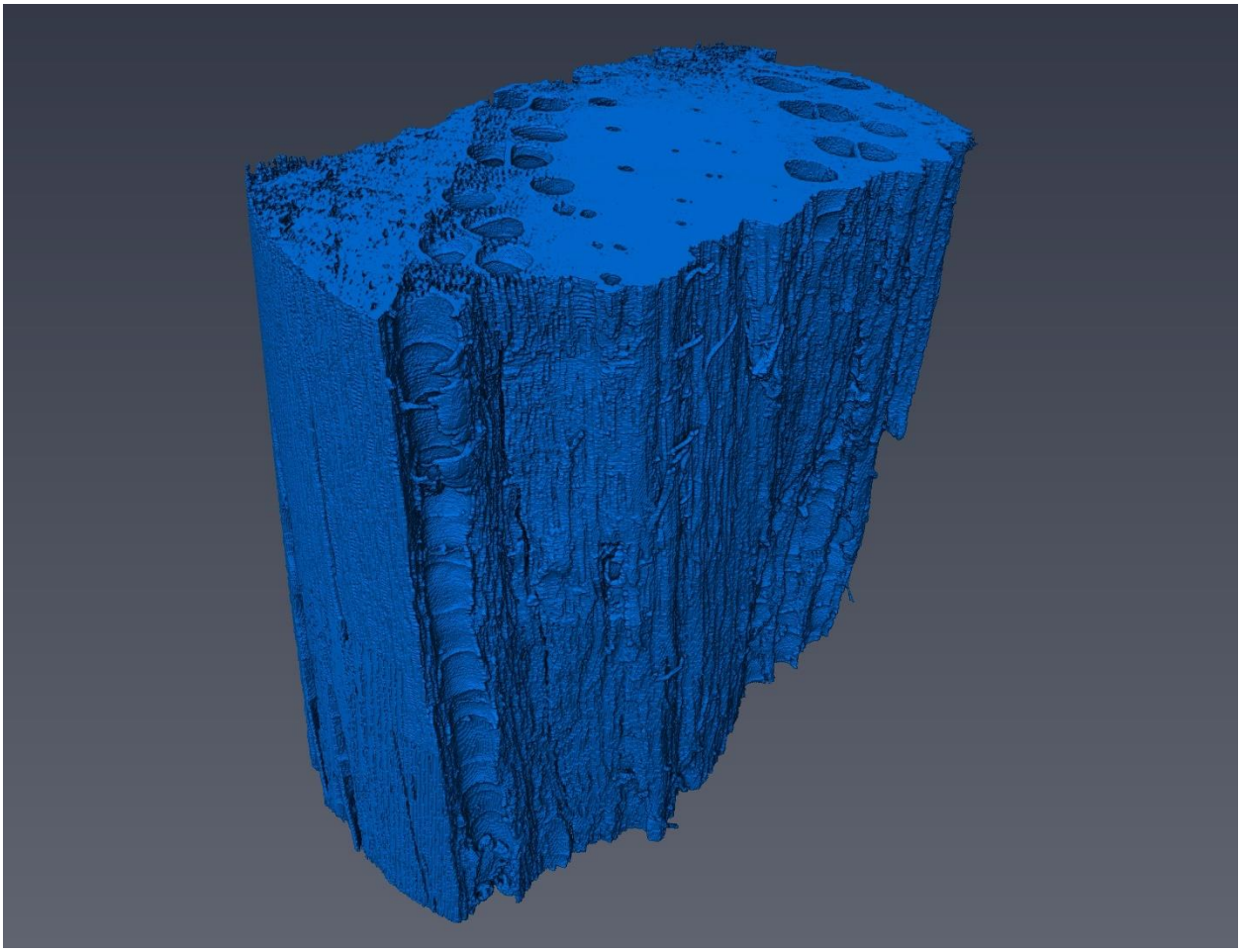

Figure S14: Three-dimensional constructed woodchip image of μCT scans. Pores can be observed at the top of the image with a partially cut-away pore seen in the foreground.

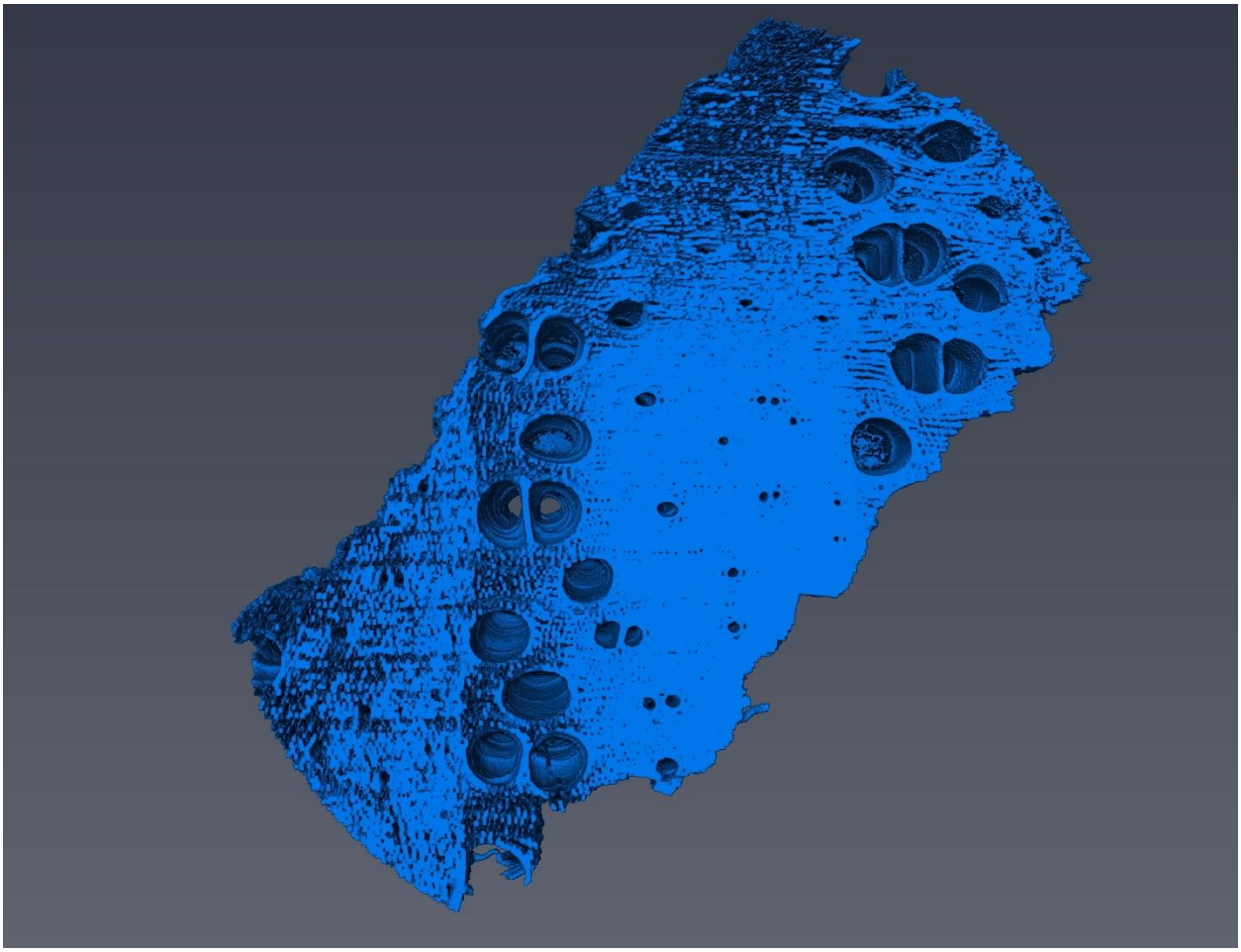

Figure S15: Three-dimensional constructed woodchip image of μCT scans. Pore "tunnels" can be seen channeling through the woodchip interior.

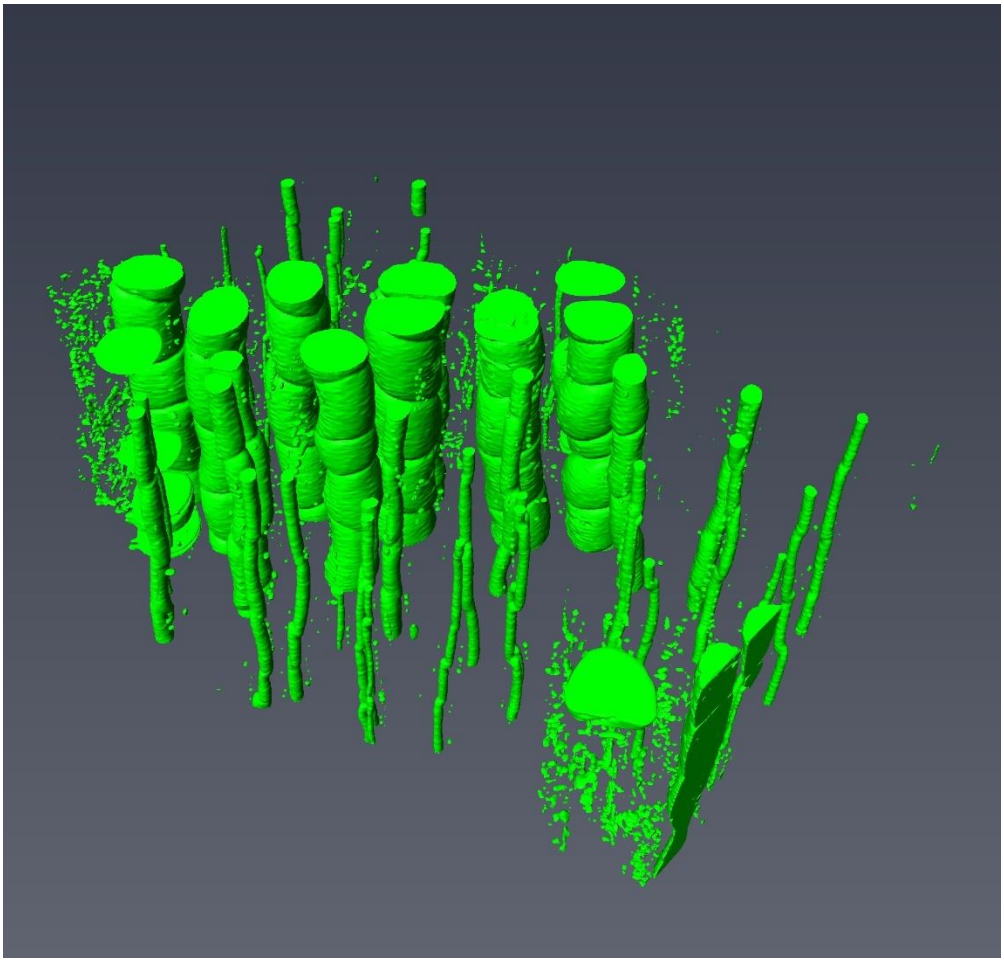

Figure S16: Three-dimensional constructed channel image of μCT scans. These "stems" indicate pore channels running through the interior of the woodchip structure.

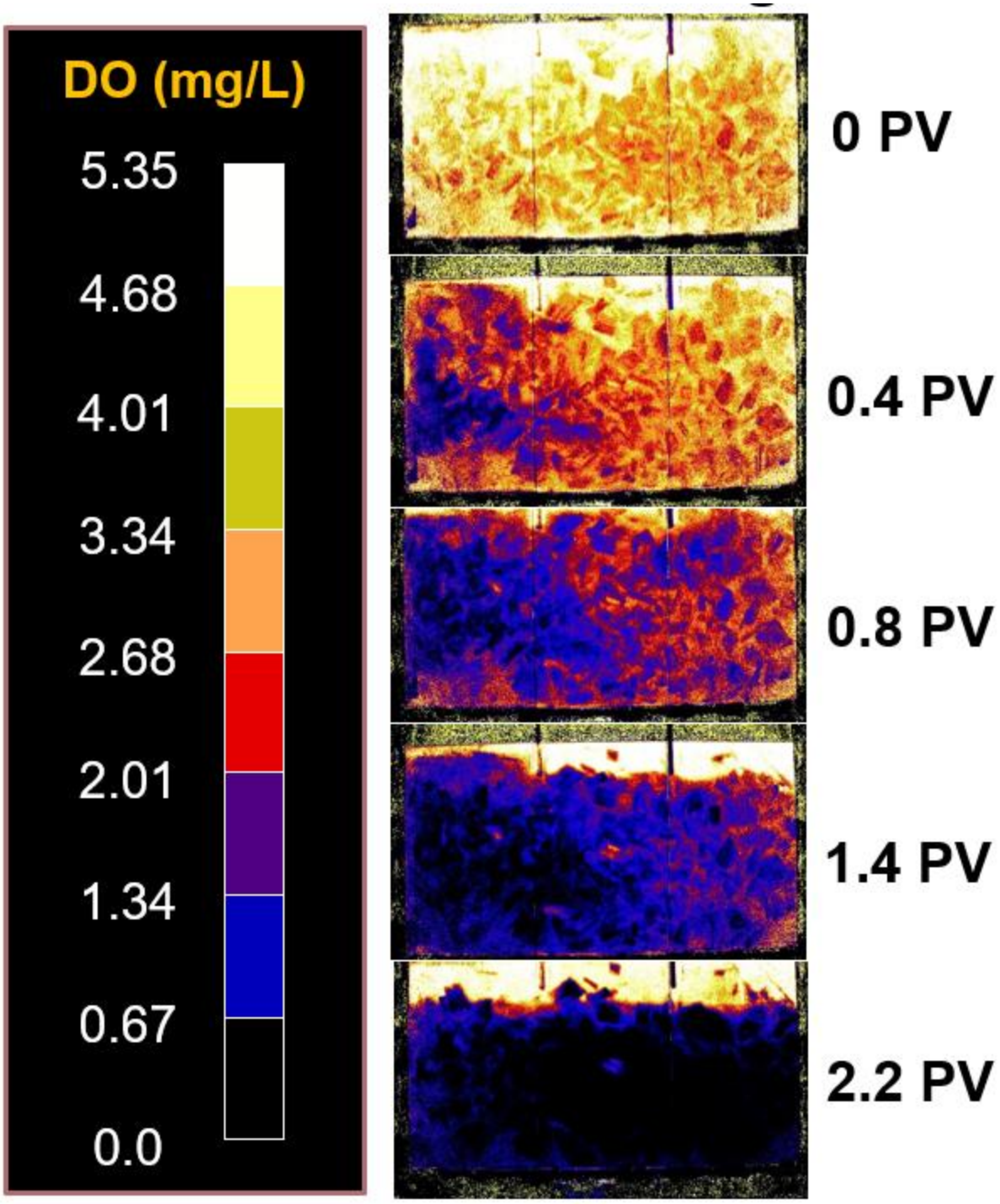

Figure S17: Reactor dissolved oxygen (DO) concentrations captured via planar optode within biotic experiment. As the oxygen depleted tracer solution is injected, DO concentrations within the reactor diminish. Biologically active woodchip media is a "hotspot" of DO consumption in early timepoints (0-0.8 pore volumes).

(1) Fry, V. A.; Istok, J. D.; Semprini, L.; O'Reilly, K. T.; Buscheck, T. E. Retardation of Dissolved Oxygen Due to a Trapped Gas Phase in Porous Media. *Groundwater* **1995**. https://doi.org/10.1111/j.1745-6584.1995.tb00295.x.

(2) Vulava, V. M.; Perry, E. B.; Romanek, C. S.; Seaman, J. C. Dissolved Gases as Partitioning Tracers for Determination of Hydrogeological Parameters. *Environ. Sci. Technol.* **2002**. https://doi.org/10.1021/es0107024.

(3) Aeschbach-Hertig, W.; El-Gamal, H.; Wieser, M.; Palcsu, L. Modeling Excess Air and Degassing in Groundwater by Equilibrium Partitioning with a Gas Phase. *Water Resour. Res.* **2008**. https://doi.org/10.1029/2007WR006454.

(4) Heilweil, V. M.; Solomon, D. K.; Perkins, K. S.; Ellett, K. M. Gas-Partitioning Tracer Test to Quantify Trapped Gas during Recharge. *Ground Water* **2004**. https://doi.org/10.1111/j.1745-6584.2004.tb02627.x.

(5) Clark, J. F.; Hudson, G. B.; Avisar, D. Gas Transport below Artificial Recharge Ponds: Insights from Dissolved Noble Gases and a Dual Gas (SF6and3He) Tracer Experiment. *Environ. Sci. Technol.* **2005**. https://doi.org/10.1021/es049053x.

(6) Gerke, H. H.; van Genuchten, M. T. A Dual-porosity Model for Simulating the Preferential Movement of Water and Solutes in Structured Porous Media. *Water Resour. Res.* **1993**. https://doi.org/10.1029/92WR02339.

(7) Jaynes, D. B.; Moorman, T. B.; Parkin, T. B.; Kaspar, T. C. Simulating Woodchip Bioreactor Performance Using a Dual-Porosity Model. *J. Environ. Qual.* **2016**. https://doi.org/10.2134/jeq2015.07.0342.

(8) Hayduk, W.; Laudie, H. Prediction of Diffusion Coefficients for Nonelectrolytes in Dilute Aqueous Solutions. *AIChE J.* **1974**. https://doi.org/10.1002/aic.690200329.

(9) King, D. B.; Saltzman, E. S. Measurement of the Diffusion Coefficient of Sulfur Hexafluoride in Water. *J. Geophys. Res.* **1995**. https://doi.org/10.1029/94JC03313.

(10) Wilhelm, E.; Battino, R.; Wilcock, R. J. Low-Pressure Solubility of Gases in Liquid Water. *Chem. Rev.* **1977**. https://doi.org/10.1021/cr60306a003.